Ordered and Disordered Phases Coexist in Plasma Membrane Vesicles of RBL-2H3 Mast Cells. An ESR Study

Mingtao Ge, Arun Gidwani, H. Alex Brown, David Holowka, Barbara Baird, and Jack H. Freed
Department of Chemistry and Chemical Biology, Baker Laboratory, Cornell University, Ithaca, New York 14853

ABSTRACT Four chain spin labels and a spin-labeled cholestane were used to study the dynamic structure of plasma membrane vesicles (PMV) prepared from RBL-2H3 mast cells at temperatures ranging from 22°C to 45°C. Analysis shows that the spectra from most labels consist of two components. The abundant spectral components exhibit substantial ordering that is intermediate between that of a liquid-ordered (Lo) phase, and that of a liquid-crystalline (Lc) phase as represented by model membranes. Also, rotational diffusion rates of the spin labels are comparable to those in the Lo phase. In contrast, the ordering for the less abundant components is much lower. These results indicate that a Lo-like region or phase (the abundant component) and an Lc-like region or phase (the less abundant component) coexist in the PMV. In contrast, membranes reconstituted from extracted lipids exhibit the more ordered phase only. This suggests that membrane-associated proteins are important for the coexistence of Lo-like and Lc-like regions in the plasma membrane. In addition, binding of the myristoylated protein, ARF6 to PMV, leads to a new spectral component for a headgroup lipid spin label that indicates the formation of plasma membrane defects by this low molecular weight GTPase.

INTRODUCTION

Microdomains in plasma membranes enriched in glycosphingolipids, cholesterol, and GPI-linked proteins, which are commonly called DRM or lipid rafts, play an important role in cell signal transduction (Simons and Toomre, 2000; Sedwick and Altman, 2002). Field et al. (1995, 1997) found that DRMs are involved in IgE receptor signaling in RBL-2H3 mast cells. Using electron spin resonance (ESR) spin labeling, we showed that DRMs isolated from detergent lysates of RBL-2H3 mast cells have a liquid-like mobility in both the acyl chain and headgroup regions and a gel-like ordering in the acyl chain region; that is, they are liquid-ordered (Ge et al., 1999). Mass spectrometric determination of the phospholipid composition of DRMs (Fridriksson et al., 1999) and fluorescence anisotropy measurements (Gidwani et al., 2001) are consistent with this conclusion. Recent studies have demonstrated that liquid-ordered and liquid-crystalline regions can coexist as distinct phases in large, unilamellar vesicles made from either model membranes or isolated plasma membrane lipids (Dietrich et al., 2001; Samsonov et al., 2001). In addition, single-particle tracking studies have indicated the existence of discrete plasma membrane domains with properties consistent with those of liquid-ordered rafts (Sheets et al., 1997; Pralle et al., 2000; Dietrich et al., 2002). These various studies provide evidence for plasma membrane heterogeneity that may depend, at least in part, on phase separation between liquid-ordered and liquid-crystalline regions; however, direct evidence for such lateral phase separation in plasma membranes is currently lacking, nor is there as yet detailed description of their dynamic structures.

The present experiments extend our ESR measurements to the plasma membrane vesicles of RBL-2H3 cells, which are prepared by chemically induced vesiculation from RBL-2H3 cells (Holowka and Baird, 1983; Gidwani et al., 2001). ESR spectra from four different spin-labeled phosphatidylcholines and a spin-labeled cholestane in the plasma membrane vesicles show that phases coexist in the membranes, which may be described as liquid-ordered-like and liquid-crystalline-like. Interestingly, ESR spectra of the same spin labels in vesicles prepared from the lipid extractions of the plasma membrane preparation only show the liquid-ordered-like-phase. No components of the liquid-crystalline-like phase could be resolved in these lipid extractions. We discuss the implications of these results. Furthermore, we observe that the binding of myr-ARF6 to the plasma membrane vesicles induces defects in the membranes, consistent with our previous suggestions from studies on model membranes that specific interactions between myr-ARF6 and PIP_2 create defects in lipid bilayers (Ge et al., 2001).

Our results indicate that a large percentage of the plasma membrane is in a liquid-ordered-like phase, but proteins confer a distinct less-ordered and more fluid phase detected by spin labels at intermediate positions on acyl chains of phospholipid derivatives.

Submitted November 20, 2002, and accepted for publication April 1, 2003.

Address reprint request to Dr. Jack H. Freed, Dept. of Chemistry and Chemical Biology, Baker Laboratory, Cornell University, Ithaca, NY 14853-1301. E-mail: jhf@ccmr.cornell.edu.

H. Alan Brown's present address is Dept. of Pharmacology, Vanderbilt University Medical Center, Nashville, TN 37232.

Abbreviations used: GPI, glycosylphosphatidylinositol; Chol, cholesterol; CSL, 3β-doxyl-5α-cholestane; DRM, detergent resistant membranes; DPPC, 1,2-dipalmitoylphosphatidylcholine; DPPTC, 1,2-dipalmitoylphospho(TEMPO) choline; TEMPO, 2,2,6,6-tetramethyl-piperidine-1-oxy; myr-ARF6, myristolyated ADP ribosylation factor 6; NLLS, nonlinear least-squares; PIP_2, phosphatidylinositol 4,5-biphosphate; POPC, 1-palmitoyl-2-oleoyl-phosphatidylcholine; SM, sphingomyelin.

0006-3495/03/08/1278/11 $2.00

MATERIALS AND METHODS

Materials

The spin labels 5PC, 7PC, 10PC, 16PC, and DPPTC were purchased from Avanti (Alabaster, AL), and CSL was from Sigma (St. Louis, MO). The expression and purification of ARF6 were performed as described previously (Ge et al., 2001).

Sample preparations

Plasma membrane vesicles were prepared according to Gidwani et al. (2001). To each plasma membrane vesicle sample (2.5×10^7 cell equivalents/0.5 ml phosphate-buffered saline pH 7.0, PBS), 25 μl of 0.07 mM spin label in methanol was added. The labeled vesicles were vortexed for 1 min and centrifuged in a Sorvall SL050T rotor at $27{,}000 \times g$ for 45 min at 4°C. The pellet was transferred to a capillary tube for ESR measurement.

Lipid extractions from plasma membrane vesicles were carried out as described by Gidwani et al. (2001). Spin-labeled lipids were added before removal of the extraction solvent (chloroform/methanol = 1/1). The molar ratio of spin label to total lipids is <0.5 mol %. The extracted lipids were dried overnight under vacuum to remove all traces of solvent. They were then hydrated in phosphate-buffered saline for 2 h, and centrifuged at 49,000 rpm at 4°C in a SW60 rotor (Beckman Instrument, Palo Alto, CA) for 45 min. The reconstituted lipid vesicles contained in the pellet were transferred to a capillary for ESR measurement.

ESR spectroscopy and NLLS fitting of ESR spectra

ESR spectra were obtained on a Bruker Instruments (Bruker Biospin Corporation, Billerica, MA) EMX ESR spectrometer at a frequency of 9.34 GHz. The NLLS analyses of the spectra were performed using the latest version of the ESR fitting program (Budil et al., 1996). Convergence to the best fit is achieved by minimizing χ^2. They yield the following parameters: rotational diffusion rate, $R_\perp$, and order parameters, S_0 and S_2. $R_\perp$ is the rotational rate of the nitroxide radical around an axis perpendicular to the mean symmetry axis for the rotation. This symmetry axis is also the direction of preferential orientation of the spin-labeled molecule (Schneider and Freed, 1989). For 5PC, 7PC, 10PC, and 16PC, $R_\perp$ represents the rotational motion of the segment in the acyl chain where the nitroxide radical is attached (Ge et al., 1994). The spectral analysis also yields $R_\parallel$, which relates to the motion about the symmetry axis. In general, the spectra are not very sensitive to $R_\parallel$, especially since $R_\parallel \gg R_\perp$. So we obtained initial estimates of $N \equiv R_\parallel/R_\perp$ and fixed N in the final fits (Ge and Freed, 1999). In the CSL molecule, the nitroxide radical is attached to the rigid fused rings, therefore $R_\perp$ represents the wagging motion of that rigid part of the CSL molecule, and again $N \gg 1$. The order parameter S_0 is a measure of the angular extent of the rotational diffusion of the nitroxide moiety relative to the membrane director. The larger the S_0, the more restricted is the motion, which usually means that laterally the lipid molecules surrounding the nitroxide radical are packed more tightly. The S_2 is the nonsymmetric order parameter, which represents the nonaxiality of the preferential orientation of the spin-labeled molecule relative to the membrane director. That is, the restriction of the wagging motion of the spin label need not be symmetric about its main symmetry axis. In addition, the NLLS analysis is effective in distinguishing more than one component when present in the spectrum. Aside from visual inspection of the detailed features of the spectrum, the NLLS analysis provides the reduced χ^2, or $\chi^2_{\text{red}} \equiv \chi^2/(n - p)$ (where n is the number of spectral points and p is the number of fitting parameters), which has been found to provide a fairly strict criterion for quality of fit (Budil et al., 1996). The χ^2_{red} is used to judge the quality of fit of one versus two or more spectral components in the present study. The best fit will yield a value for χ^2_{red} closest to unity.

ARF6 binding to the plasma membrane vesicles

After the ESR spectrum of DPPTC in the plasma membrane vesicles (before adding ARF6) was taken, 10 μl of ARF6 solution (0.43 mg/ml) was added to the capillary tube. To mix the vesicles with ARF6 properly, the capillary was sealed, placed inverted in a desktop centrifuge, and spun for 2 min. An ESR spectrum from the vesicle bound with ARF6 was taken. In the same manner, more ARF6 was added and mixed with the vesicles, and then ESR spectra were taken. Before adding the additional ARF6, some of the supernatant in the capillary had to be removed to make space for the new ARF6 solution.

RESULTS AND DISCUSSION

Plotted in Fig. 1 are ESR spectra from spin labels 5PC, 7PC, 10PC, 16PC, and CSL in the plasma membrane vesicles and in the lipid vesicles reconstituted from extracted lipids, over the temperature range of 22–45°C. The solid lines are experimental spectra and the dashed lines superimposed are the least-squares fits. It is seen that for all cases the agreement between the experimental and the fitted spectra is very good. The spectra of 5PC, 7PC, and 10PC in the plasma membrane vesicles could not be fit satisfactorily with just a single component, but are well-fit with two components as we discuss further. However, the 16PC and CSL spectra in Fig. 1 were well-fit with only a single component. The two-component fit for the spectrum of 5PC in the plasma membrane vesicles at 22°C is illustrated in Fig. 2, where the experimental spectrum (*solid line* in Fig. 2 *A*) and the two-component fit (*dotted* line in Fig. 2 *A*) are compared with the experimental spectrum (*solid line* in Fig. 2 *B*) and the successful one-component fit (*dotted line* in Fig. 2 *B*) from the lipid extraction of the plasma membrane. We discuss the implications of the fact that the lipid extract yields only a single component in a later subsection. We include it here for comparison to clarify the issue of distinguishing two components versus one component in these ESR spectra. The two components obtained from the fit to the plasma membrane vesicle spectrum in Fig. 2 *A* are shown in Fig. 2, *C* and *D*. Also for comparison, we show in Fig. 2 *E* the best single component fit (*dotted lines*) to the experimental spectrum from Fig. 2 *A* (*solid line*). Clearly this is a less satisfactory fit. There are two regions in the spectrum, to the left and to the right of center, which are particularly sensitive to the presence of the single component. Enlarged (by 3×) insets are provided in Fig. 2, *A*, *B*, and *E*, to show how well the best fit spectra compare with their corresponding experimental spectra in these regions. Characteristic ''two-component'' features of the ESR spectrum are shown in the insets to Fig. 2 *A* with arrows pointing to the effect of the second component shown in Fig. 2 *D*. Neither the best one-component fit, shown in Fig. 2 *E*, nor the good single-component spectrum and fit, shown in Fig. 2 *B*, for the lipid extracts display these features. Thus, the NLLS fitting procedure clearly discriminated the need to use the two components for the spectrum in Fig. 2 *A*, whereas it successfully returned only a single component in fitting

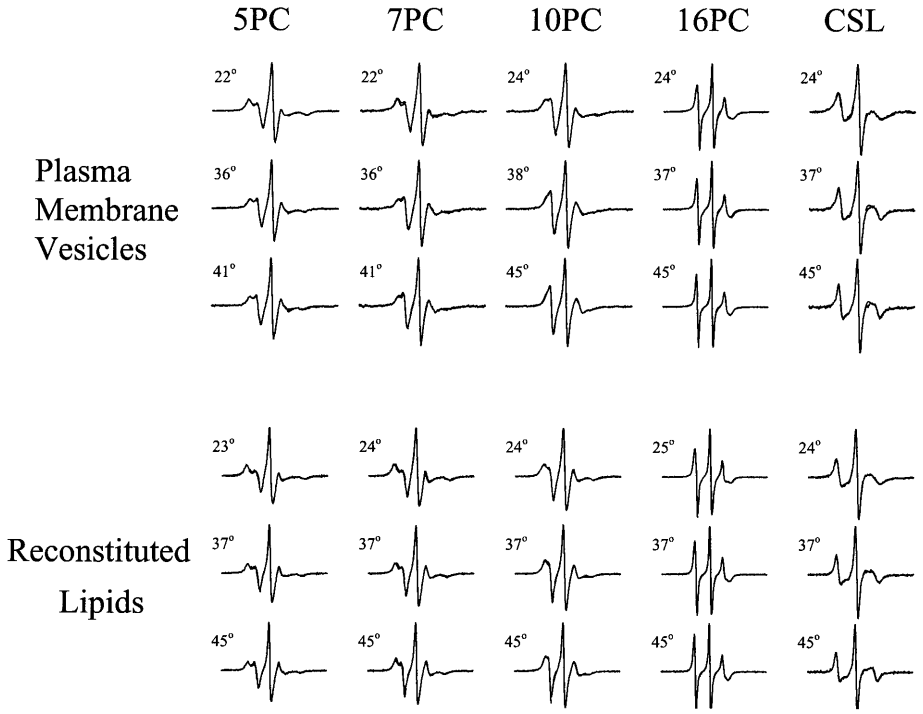

FIGURE 1 ESR spectra of spin labels 5PC, 7PC, 10PC, 16PC, and CSL in the plasma membrane vesicles and the reconstituted lipids at various temperatures.

Fig. 2 *B*, rejecting the need for any second component. (Spectral subtraction between the experimental spectra in Fig. 2, *A* and *B*, does show the presence of the second component in the former, although it does not completely remove the first component. This is expected because of small but significant differences in spectral features of this component in Fig. 2, *A* and *B*. These are reflected in the small differences in $R_\perp$, S_0, and S_2 found for the plasma membrane vesicles in Table 1 versus those found for the lipid extracts in Table 2.)

Of the various statistics provided in the NLLS fitting package, the reduced χ^2 (or χ^2_{red}) described in ''Materials and Methods'' provides a good objective criterion for quality of fit. For the fit in Fig. 2 *A*, $\chi^2_{\text{red}} = 5.8$, which is definitely superior to the $\chi^2_{\text{red}} = 29$ for the fit in Fig. 2 *E*. (This is especially significant in view of the fact that the χ^2_{red} is heavily affected by the intense central region of the spectrum, which is not sensitive to whether one or two components are used). This confirms the need for the two-component fit in Fig. 2 *A*. Similar considerations apply to the plasma membrane vesicle spectra from 7PC and 10PC, which also required two components to obtain goods fits, whereas those from 16PC and CSL were found by the NLLS procedure to require only a single component.

The best NLLS parameters of rotational diffusion rate, $R_\perp$, order parameters, S_0 and S_2, and populations of the two components of the ESR spectra from the plasma membrane vesicles are listed in Table 1. The best NLLS parameters of $R_\perp$, S_0, and S_2 for ESR spectra from the reconstituted lipid vesicles are listed in Table 2. In Fig. 3, the best fit values of S_0 for CSL, 5PC, 7PC, 10PC, and 16PC in plasma membrane vesicles are plotted versus the temperature. For 5PC, 7PC, and 10PC, the values of S_0 are those for component 1. For comparison, the S_0 from CSL in pure SM at 37°C (gel phase) and 50°C (liquid-crystalline phase), from 5PC in DRM at 22°C, and from 16PC in DRM, DPPC/Chol of molar ratio 1/1 (abbreviated as DPCH) and 16PC in pure DPPC are also plotted (Ge et al., 1999). The rotational diffusion rates in plasma membrane vesicles are plotted in Fig. 4 *A* (CSL), *B* (component 1 of spectra from 5PC, 7PC, and 10PC), and *C* (16PC) versus the temperature. Also, for comparison, the rotational diffusion rates of CSL in pure SM (Fig. 4 *A*), of 5PC in DRM (Fig. 4 *B*), and of 16PC in DRM, pure DPPC, and in DPCH (Fig. 4 *C*) are plotted. The comparisons with results in these model systems given below provide better insight into the interpretation of the results on the plasma membrane vesicles.

Coexisting phases in plasma membrane vesicles

The distinct values of $R_\perp$ and S_0 of the two components for ESR spectra of 5PC, 7PC, and 10PC in the plasma membrane vesicles indicate that two different membrane structures coexist in these vesicles. As shown in Table 1, the relative populations of the two components do not vary significantly with temperature. (However, the population of component 1 in 10PC spectra decreases with temperature as described in more detail below.) The average percentage of component 1 of the spectra from 5PC and 7PC over the three temperatures is 89%. In later discussion, component 1 is

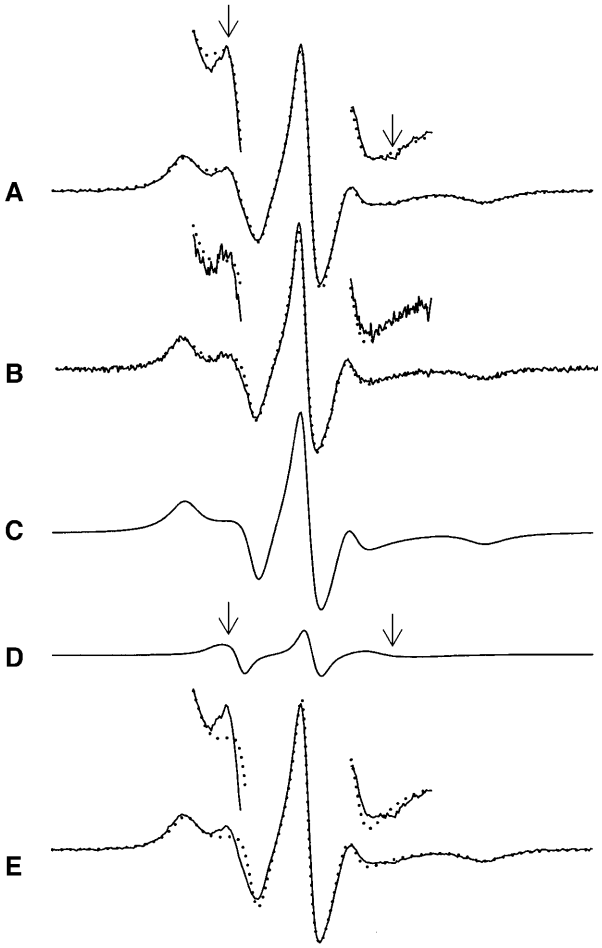

FIGURE 2 Experimental spectrum (*A*, *solid line*), simulation (*A*, *dotted line*), and the calculated two components (*C* and *D*) by NLLS analysis for 5PC in the plasma membrane vesicles at 22°C, with the results for 5PC in the reconstituted lipids at 23°C shown in *B*. Arrows point to the second component feature *A* (and *D*) that are not present in *B*. *E* (*dotted line*) is the simulation from one-component fit for 5PC in the plasma membrane vesicles, and *E* (*solid line*) is the corresponding experimental spectrum, which is the same as *A* (*solid line*).

TABLE 1 Parameters obtained from NLLS fitting of ESR spectra of various spin labels in plasma membrane vesicles

	T(°C)	C*	$R_\perp(s^{-1})$	S_0	S_2	P*
5PC	22	1	3.98×10^7	0.42	−0.23	0.87
		2	7.41×10^7	0.24	−0.40	0.13
	36	1	6.17×10^7	0.39	−0.19	0.91
		2	1.32×10^8	0.20	−0.26	0.09
	41	1	7.59×10^7	0.41	−0.18	0.89
		2	1.38×10^8	0.20	−0.26	0.11
7PC	22	1	4.57×10^7	0.38	−0.21	0.92
		2	9.33×10^7	0.17	−0.17	0.08
	36	1	6.17×10^7	0.37	−0.19	0.87
		2	1.26×10^8	0.19	−0.30	0.13
	41	1	6.76×10^7	0.35	−0.19	0.87
		2	1.38×10^8	0.16	−0.08	0.13
10PC	24	1	4.57×10^7	0.31	−0.22	0.89
		2	8.71×10^7	0.13	−0.10	0.11
	38	1	8.71×10^7	0.33	−0.18	0.79
		2	1.02×10^8	0.11	−0.03	0.21
	45	1	9.77×10^7	0.31	−0.19	0.76
		2	1.20×10^8	0.11	−0.04	0.24
16PC	24		2.51×10^8	0.17	−0.15	
	37		2.69×10^8	0.13	−0.13	
	45		3.31×10^8	0.12	−0.14	
CSL	24		1.82×10^7	0.91	0.03	
	37		4.90×10^7	0.85	0.06	
	45		5.01×10^7	0.78	0.11	

Magnetic parameters used in the simulations are
5PC: $g_{xx} = 2.0080$, $g_{yy} = 2.0058$, $g_{zz} = 2.0022$; $A_{xx} = 5.75$ G, $A_{yy} = 5.75$ G, $A_{zz} = 33.50$ G.
7PC: $g_{xx} = 2.0082$, $g_{yy} = 2.0062$, $g_{zz} = 2.0020$; $A_{xx} = 5.50$ G, $A_{yy} = 5.50$ G, $A_{zz} = 33.30$ G.
10PC: $g_{xx} = 2.0084$, $g_{yy} = 2.0062$, $g_{zz} = 2.0020$; $A_{xx} = 5.40$ G, $A_{yy} = 5.40$ G, $A_{zz} = 33.50$ G.
16PC: $g_{xx} = 2.0082$, $g_{yy} = 2.0062$, $g_{zz} = 2.0020$; $A_{xx} = 5.50$ G, $A_{yy} = 5.50$ G, $A_{zz} = 33.30$ G.
CSL: $g_{xx} = 2.0082$, $g_{yy} = 2.0057$, $g_{zz} = 2.0020$; $A_{xx} = 5.80$ G, $A_{yy} = 5.80$ G, $A_{zz} = 34.00$ G.

Error estimates in the parameters were obtained from the NLLS fitting as described in Budil et al. (1996). Here we give average errors for compactness in presentation: $R_\perp$, ± 5%; S_0, ± 0.02; S_2, ± 0.05; P, ± 5.0%.
*C, component; P, population.

referred to as the more abundant membrane component, and component 2 the less abundant component. Since the population of component 1 is much larger than the population of component 2 for 5PC, 7PC, and 10PC spectra, we expect that the ESR spectra from 16PC and CSL (one component) must be predominantly from spin labels located in the more abundant component in the plasma membrane.

1. Let us examine the ordering and dynamics of the acyl chains in the more abundant component. From Fig. 3, we found the following features: 1), The order parameter, S_0, of 16PC in the plasma membrane vesicles, which ranges from 0.17 (22°C) to 0.12 (45°C), is smaller than that in DRM, which ranges from 0.23 (24°C) to 0.19 (45°C). Also it is smaller than the S_0 in DPCH, which is constant over the temperature range from 25°C to 45°C, i.e., 0.22. We previously presented evidence that DRM has a liquid-ordered phase structure similar to that of DPCH (Ge et al., 1999). Although the S_0 of 16PC in plasma membrane vesicles is smaller than in DPCH and DRM, it is still larger than that of 16PC in pure DPPC in both gel and liquid-crystalline phases. In the latter case, S_0 decreases from 0.13 at 30°C to 0.06 at 40°C in the gel phase, and sharply drops to nearly zero at 41°C, the gel to liquid-crystalline phase transition temperature.
2. S_0 for 5PC in the plasma membrane vesicles, ~0.41, remains nearly unchanged from 22°C to 41°C. It is larger than S_0 of 5PC in SM in the liquid-crystalline phase, i.e., 0.37 at 50°C, but is smaller than S_0 of 5PC in SM in the gel phase, i.e., 0.46 at 20°C. It is also significantly smaller than S_0 of 5PC in DRM at 22°C, i.e., 0.52.

TABLE 2 Parameters obtained from NLLS fitting of ESR spectra of various spin labels in reconstituted lipid vesicles from plasma membranes

	T(°C)	$R_\perp(s^{-1})$	S_0	S_2
5PC	23	3.80×10^7	0.38	−0.21
	37	5.62×10^7	0.38	−0.17
	45	6.17×10^7	0.34	0.02
7PC	24	4.68×10^7	0.39	−0.20
	37	6.46×10^7	0.38	0.05
	45	1.26×10^8	0.37	0.07
10PC	24	5.13×10^7	0.32	0.06
	37	8.91×10^7	0.29	0.10
	45	1.16×10^8	0.28	−0.02
16PC	25	3.09×10^8	0.18	−0.20
	37	3.16×10^8	0.15	−0.20
	45	3.47×10^8	0.13	−0.20
CSL	24	7.08×10^7	0.91	0.01
	37	8.71×10^7	0.85	0.05
	45	1.26×10^8	0.82	0.06

The magnetic parameters used in the simulations are the same as listed in first footnote of Table 1. For error estimates, see legend of Table l.

The above results (1) and (2) for the S_0 of 5PC and 16PC in plasma membrane vesicles are consistent with recent fluorescence anisotropy measurements with diphenylhexatriene-PC of acyl chain ordering in the plasma membrane vesicles derived from RBL-2H3 cells (Gidwani et al., 2001). They found that ordering of the acyl chain in plasma membrane vesicles is lower than in DRM and DPPC + 33 mol % Chol vesicles (100% liquid-ordered phase), but is higher than that in pure POPC vesicles.

3. At 37°C, the S_0 of CSL in the plasma membrane vesicles, 0.85, is the same as that in DRM at the same temperature. This is not only much larger than the S_0 of all the chain spin labels in the plasma membrane vesicles, but also much larger than S_0 of CSL in SM, i.e., 0.53 at 37°C (gel phase) and 0.49 at 50°C (liquid-crystalline phase). In addition, S_0 of CSL has the largest temperature coefficient. That is, the S_0 in plasma membrane vesicles decreases by 0.13 from 0.91 at 24°C to 0.78 at 45°C. In the same temperature range, S_0 of 5PC and 10PC remain nearly unchanged, and S_0 of 7PC decreases only by 0.03 from 0.38 at 22°C to 0.35 at 41°C. We attribute these features of ordering of CSL to the structure of the CSL molecule, wherein the nitroxide radical is rigidly attached to the rigid ring structure of cholestane. This makes the CSL molecule more sensitive to constraints of molecular packing in its surroundings than the chain spin labels.
4. In plasma membrane vesicles, the S_0 of all the spin labels we used in this work varies with the temperature smoothly and gradually. In contrast, there is a sharp drop in the S_0 of 16PC in DPPC at 41°C, the gel to liquid-crystalline phase transition temperature.

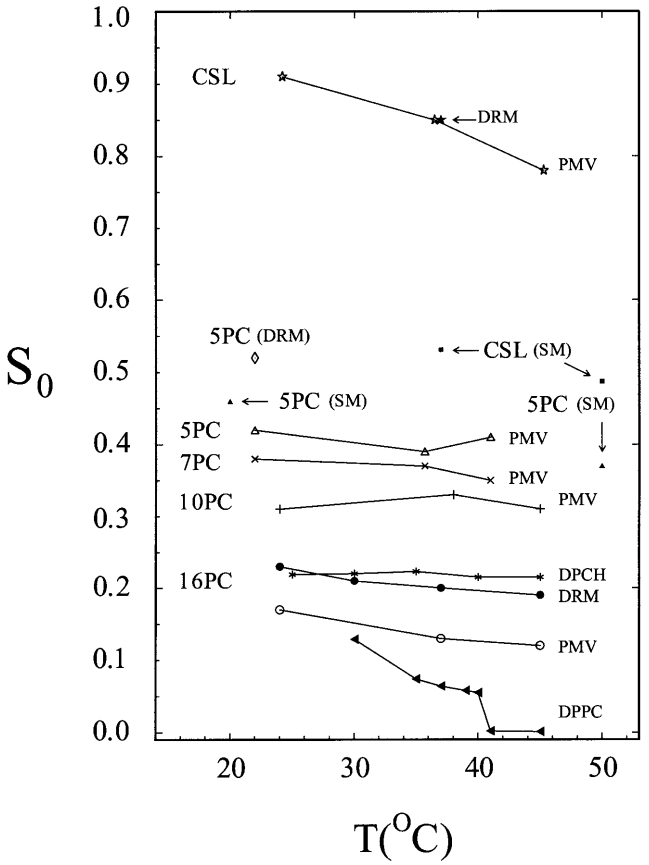

FIGURE 3 Plot of best-fit values of the order parameter S_0 of CSL, 5PC, 7PC, 10PC, and 16PC in the plasma membrane vesicles (PMV) versus the temperature. For 5PC, 7PC, and 10PC, the values of S_0 are those of component 1 in the two-component fit. The order parameters of the following spin labels are also plotted: CSL and 5PC in pure SM and DRM; 16PC in pure DPPC, DRM, and DPPC/Chol = 1/1 (DPCH).

5. All the chain spin labels in the plasma membrane vesicles show relatively large negative S_2, whereas the S_2 values of CSL is very small and positive (cf. Table 1). The axial ordering of CSL is characteristic of this rigid, cigar-shaped molecule and has been observed in previous studies (Freed, 1994; Freed et al., 1994). The substantial negative S_2s of the acyl chains reflect the composite effects of their more complex motions including both (restricted) overall tumbling and internal chain dynamics (Lou et al., 2001).

The features in the rotational diffusion rates, $R_\perp$, of those spin labels in the more abundant plasma membrane component can be summarized as follows. As shown in Fig. 4 *B*, the $R_\perp$s of 5PC (of component 1) in the plasma membrane vesicles and in DRM at 22°C are nearly equal ($\sim 4.0 \times 10^7$ s^{-1}), but greater than that of 5PC in the gel phase of SM at 20°C, 1.62×10^7 s^{-1} (Ge et al., 1999). The $R_\perp$ of 5PC in the more abundant plasma membrane component at 41°C, 7.59×10^7 s^{-1}, is slightly greater than

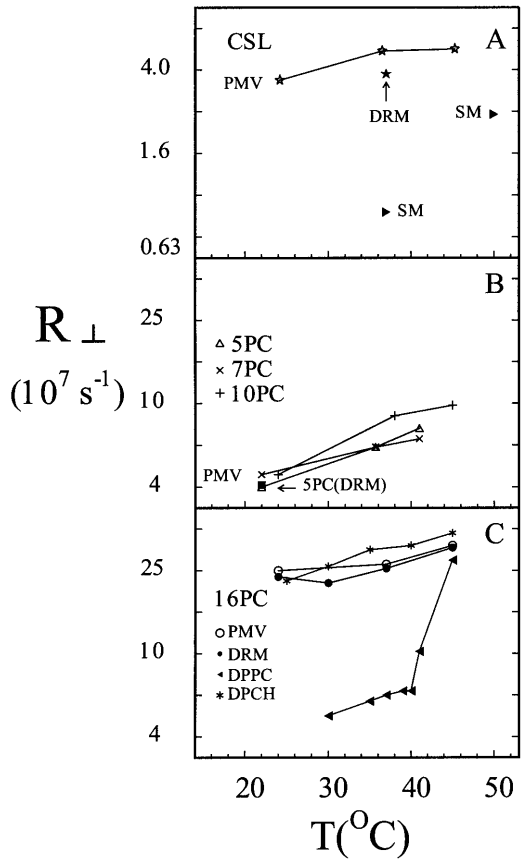

FIGURE 4 Plots of best-fit values of the rotational diffusion rate $R_\perp$ of CSL (*A*), 5PC, 7PC, and 10PC (*B*), and 16PC (*C*) versus temperature in the plasma membrane vesicles (PMV). The rotational diffusion rates $R_\perp$ of the following spin labels are also plotted: (*A*) CSL in SM and DRM; (*B*) 5PC in DRM; and (*C*) 16PC in pure DPPC, DRM, and DPPC/Chol = 1/1 (DPCH).

that of 5PC in SM at 50°C (liquid-crystalline phase), 7.08×10^7 s^{-1} (Ge et al., 1999). Moreover, it is shown in Fig. 4 *A* that the $R_\perp$s of CSL in the plasma membrane vesicles, ranging from 1.82×10^7 s^{-1} (22°C) to 5.01×10^7 s^{-1} (45°C), are comparable to those in DRM (3.80×10^7 s^{-1} at 37°C). They are much higher than the $R_\perp$s of CSL in SM at 37°C (gel phase), 8.31×10^6 s^{-1}, and at 50°C (liquid-crystalline phase), 2.43×10^7 s^{-1} (Ge et al., 1999). Interestingly, between 22°C and 41°C, the $R_\perp$s of 5PC and 7PC in the more abundant component are nearly the same. They are comparable to those of CSL in the plasma membrane vesicles in the same temperature range. (The $R_\perp$s of 10PC in the plasma membrane vesicles are comparable to or slightly greater than those of 5PC, 7PC, and CSL). Since a CSL molecule can be regarded as a spin-labeled Chol molecule (Barnes and Freed, 1998, and references therein), the above results suggest that the rotational diffusion of a cholesterol molecule and the rotational diffusion of the lipid, at least in the acyl chain region above C10, (i.e., C5 and C7) experience similar frictional forces. This suggests that molecular interactions between the Chol molecule and the lipids in the more abundant component are substantial. It would also appear that with Chol present, conformational changes of the acyl chains, at least in the region above C10, are significantly suppressed.

In addition, Fig. 4 *C* shows that the rotational diffusion rates $R_\perp$ of 16 PC in the more abundant plasma membrane component that increase from 2.51×10^8 s^{-1}at 24°C to 3.31×10^8 s^{-1} at 45°C (Table 1) are comparable to those in DRM and DPCH in the same temperature range, (i.e., increasing from 2.34×10^8 s^{-1} at 24°C to 3.24×10^8 s^{-1} at 45°C for DRM, and increasing from 2.23×10^8 s^{-1}at 25°C to 3.80×10^8 s^{-1} at 45°C for DPCH). But the values of $R_\perp$ of 16PC in the gel phase DPPC (below 41°C) are less than 6.60×10^7 s^{-1}, which are much smaller than those in the plasma membrane vesicles and DRM. Only when the temperature is above 45°C is the $R_\perp$ of 16PC in DPPC (liquid-crystalline phase) comparable to those in the abundant membrane of the plasma membrane vesicles and in DRM. Therefore, the end chain segments in plasma membrane vesicles are also as mobile as in the liquid-ordered phase.

In summary, for the more abundant component, the ordering of the acyl chains in the plasma membrane is lower than that in DRM and DPCH, but is higher than for pure phospholipids such as DPPC and SM below their phase transition; the rotational diffusion rate of acyl chains is nearly the same as for DRM and DPCH, but is larger than for pure phospholipids. Thus, the more abundant component is in a phase that has properties quite similar to that of a liquid-ordered phase despite its somewhat reduced ordering.

In the plasma membrane vesicles, acyl chains in the less abundant component have larger $R_\perp$ but much lower S_0 than acyl chains in the more abundant component. The S_0 of 5PC for the less abundant component at 41°C, 0.20, is even lower than S_0 of 5PC in the liquid-crystalline phase of SM at 50°C, 0.37. Thus we can describe the less abundant component as being in a liquid-crystalline (Lc)-like phase, which coexists with the liquid-ordered (Lo)-like phase of the more abundant component. However, this less abundant component exhibits no phase transition characteristic of pure lipids over the temperature ranges studied as we would expect for a membrane containing a wide mixture of lipids, wherein there is a wide variation in their transition temperatures in their pure forms. We point out here that the two-component ESR spectra we observed from 5PC and 16PC in DRMs isolated from RBL-2H3 cells (Ge et al., 1999) are somewhat different from the two components in the ESR spectra from the plasma membrane vesicles. In the former case, one component is a typical spectrum from a Lo phase, but the other one is severely broadened, most likely due to clustering of spin labels. We were unable to identify the phase structure of the second component in this case.

We have already noted that our results for 5PC, 7PC, (and 10PC at 22°C) yielded a population of ~11% for the less

abundant component. There are two issues that require discussion here. First is the question of the relative populations of the two coexisting phases, which is not necessarily that of the observed spectral components. For this to be the case, one needs the partition coefficient for each of the spin labels in the two phases or regions to be unity. Although it is not possible to directly determine them in the plasma membrane vesicles (PMV), one can be guided by results for two-phase systems in model membranes. Using the model system of DLPC/DPPC, which yields a two-phase region with a DLPC-rich Lc phase and a DPPC-rich gel phase (Feigenson and Buboltz, 2001), we found that 16PC partitions equally (i.e., 1:1), whereas 5PC partitions ~3:1 with a preference for the DLPC-rich Lc phase (Y. W. Jiang, J. T. Buboltz, G. W. Feigenson, and J. H. Freed, unpublished results). The differences observed in the dynamic structure between Lc and gel phases are greater than the small differences found in the present study on PMV between the Lc-like and Lo-like phases. Thus, it seems reasonable that 16PC partitions about equally in the two PMV phases, whereas 5PC is at *most* ~3 times more likely to partition in the less abundant Lc-like phase. If we use this value for the partition coefficient of 5PC in the PMV phases, then we would conclude that the less abundant phase is only ~4% of the PMV. Also, the greater partitioning of 5 PC than 16PC in the Lc-like phase might be an additional reason why no second component is seen with 16PC.

Given that the less abundant component could be only ~4% (but no more than ~11%), the second question that arises is whether this can represent some impurity (e.g., intracellular membrane). Whereas the procedure for producing the PMV from RBL cells leads to samples of high purity (Holowka and Baird, 1983), this alone cannot rule out the role of an impurity. However, we found for the case of lipids extracted from the PMV (cf. Fig. 5, with further discussion below) that they yield only a single component equivalent in dynamic structural properties to the more abundant component of the PMV. This observation is, in our estimation, a significant argument implicating the role of the protein in yielding the less-abundant component in the PMV.

We further note that the ESR spectrum of 5PC from the less abundant membrane component corresponds to a highly mobile lipid population. If this component is due to an intracellular membrane (present in the PMV preparation as an impurity), then it would imply that the entire intracellular membrane component is in a highly mobile dynamic state. We think this is highly unlikely. Numerous studies of ESR spectra of 5PC in fluid lipid bilayers in a range of different phospholipids are unlike the spectrum shown in Fig. 2 *D* in that they all display significantly lower mobility (see, e.g., Ge and Freed, 1993; Ge et al., 2001; Swamy et al., 2000; Swamy and Marsh, 2001). Based upon this fact, we believe the less abundant component must be due to the effect of proteins in the plasma membranes and represents some local defect in the plasma membranes, induced by the presence of proteins wherein mobility is less restricted. This is not unlike our observations of the effects induced by ARF6 binding described below and by Ge et al. (2001).

In perhaps a related matter, it was mentioned above that the population of the second component of 10PC in the plasma membrane vesicles increases from 0.11 at 24°C to 0.24 at 45°C. This could be due to a temperature-dependent partition coefficient for 10PC, or it may be due to (additional) defect formation of the type previously observed for 10PC in pure DPPC and DSPC bilayers in a certain range of temperature (Ge et al., 2001). These defects in membranes, for which 10PC has a propensity, have a very low ordering, so that spectra from spin labels located in the defects in the plasma membrane vesicles may not be resolvable from the spectra of spin labels in the less abundant component.

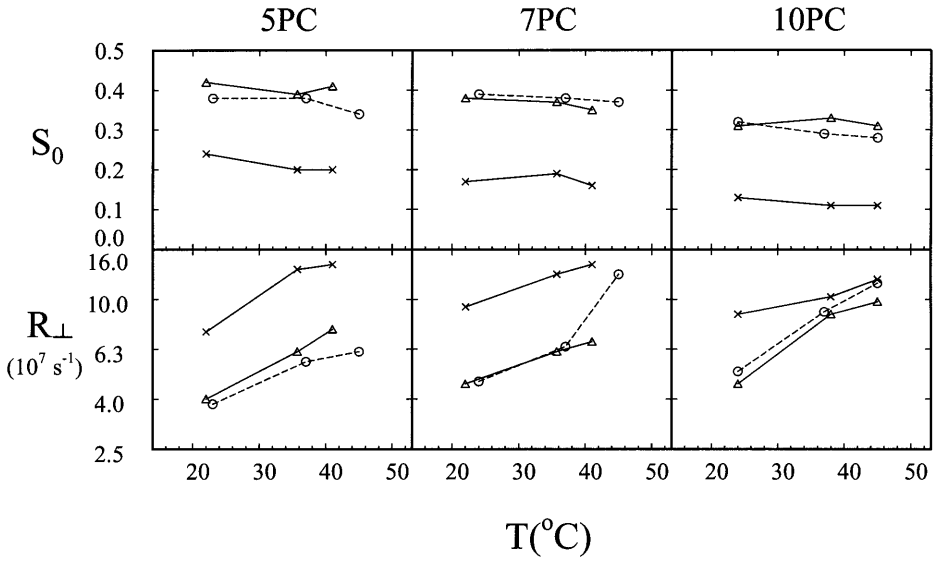

FIGURE 5 Plots of the order parameter S_0 and the rotational diffusion rate $R_\perp$ of 5PC, 7PC, and 10PC in the plasma membrane vesicles (two components, *open circle*—component 1, *cross*—component 2), and in the lipid extractions (*triangle*) versus the temperature.

The liquid-ordered-like structure of bilayers of lipids extracted from the plasma membrane vesicles

It is striking that unlike the spectra of 5PC, 7PC, and 10PC in the plasma membrane vesicles, the NLLS fits to spectra from these three chain spin labels in the reconstituted lipid vesicle did not distinguish more than one component. This was discussed above in the context of the spectrum for 5PC in the reconstituted lipids shown in Fig. 2 *B* and the comparable one from the plasma membrane in Fig. 2 *A*. We have noted that the NLLS analysis unequivocally yields only a single component in fitting Fig. 2 *B*, and other spectra from the reconstituted lipids, whereas it readily returns the two components in fitting Fig. 2 *A* and other spectra from the plasma membrane. Fig. 2 *B* is seen to be very similar (but not identical) to the spectrum from the more abundant plasma membrane component shown in Fig. 2 *C*. In Fig. 5, the best-fit parameters of $R_\perp$ and S_0 for 5PC, 7PC, and 10PC in the lipid extractions are compared with those of the same spin labels in the two components of the plasma membrane vesicles. Both parameters for the reconstituted lipid vesicles are very close to those for the more abundant component, indicating that these reconstituted lipids are primarily in the liquid-ordered phase. This implies that removal of proteins from the plasma membrane vesicles substantially reduces the liquid-crystalline-like phase from these membranes.

Consistent with this, it was shown that calcium-dependent ATPase has different binding constants for different lipids. Thus, the composition of the lipid annulus around the ATPase is different from the bulk lipid composition of the membrane (Lee, 1988). A possible mechanism for this effect is that some proteins localized in the liquid-ordered-like phase preferentially bind to sphingomyelin, and saturated and monosaturated lipids, which are known to be enriched in the plasma membrane vesicles (Fridriksson et al., 1999). This interaction stabilizes the phase separation of the Lo-like phase from the Lc-like phase in the plasma membrane vesicles, possibly with cholesterol remaining in the Lo-like phase. Perhaps more likely is the possibility that there is an Lc-like region that largely represents the annulus of lipid around transmembrane proteins in the plasma membrane, and this lipid may remain bound to protein or else lose its more disordered character in the absence of the transmembrane protein after extraction and vesicle reconstitution.

Plasma membranes versus DRMs

DRMs have a lower protein/phospholipid ratio than the plasma membranes from which they are derived (Apgar and Mescher, 1986), and this may be a reason for the observation of the less abundant component in the plasma membranes and not in the DRMs. Also, plasma membranes contain considerably more polyunsaturated lipids than do DRMs (Fridriksson et al., 1999). It is reasonable that greater unsaturation would lead to reduced ordering of the acyl chains in the plasma membranes, consistent with our observations on the less abundant component. Also, consistent with these ESR results, fluorescence anisotropy measurements showed that the average order of the plasma membrane vesicles is somewhat less than that for isolated DRMs (Gidwani et al., 2001). Interestingly, these anisotropy measurements did not detect the less abundant component, and showed identical results for the plasma membranes and the extracted, reconstituted lipids, suggesting that the spin probes and fluorescence anisotropy probe partition differently in the more fluid phase, or perhaps the fluorescence experiment is not as sensitive a measurement.

ARF6 binding to plasma membrane vesicles induces defects in the membranes

Previously we showed that ARF6 binding to multilamellar vesicles and large unilamellar vesicles containing PIP_2 produces defects in the bilayers due to the specific interactions between ARF6 and PIP_2 (Ge et al., 2001). PIP_2 is located primarily at the inner leaflet of the plasma membrane (0.1–5% of the inner bilayer lipids (Raucher et al., 2000)), so the isolated plasma membrane vesicles may exhibit detectable perturbation as a consequence of ARF6 binding. Indeed, as shown in Fig. 6, as the amount of ARF6 that binds to the plasma membrane vesicles is increased, i.e., as the lipid/ARF6 molar ratio decreases from 600 to 200, the high-field peak of the ESR spectrum from DPPTC shows the development of a sharp spectral component. In fact, by simple subtraction of the spectrum obtained before ARF6 binding from the spectra obtained after ARF6 binding, a relatively sharp nitroxide spectrum emerges, as shown in Fig. 7. One sees that this sharper spectrum grows in intensity as ARF6 is added. By means of spectral integrations, this was quantified. We find for molar ratios of 600, 300, and 200 (of lipid/ARF6), the sharper component constitutes 2%, 6%, and 14%, respectively, of the total integrated spectrum. That is, this sharper component, which we attribute to defect formation in the membrane, grows in faster than the 1:2:3 ratio we would expect from a linear dependence on ARF6 concentration, suggestive of a cooperative effect, such as one involving ARF6-induced lipid aggregation, possibly due to ARF6 interaction with PIP_2 or other negatively charged lipids (cf. Ge et al., 2001).

Given that the difference spectrum of Fig. 7 *C* has the best signal-to-noise, we obtained a fit to it by NLLS. We found $S_0 = 0.21$ with $R_\perp = 4.7 \times 10^7\ s^{-1}$. This may be compared with values for DPPTC obtained previously in model membranes, with dioleoylphosphatidyl-ethanolamine as the predominant component but also containing PIP_2 (Ge et al., 2001). They were $S_0 = 0.23$ and $R_\perp = 2.0 \times 10^8\ s^{-1}$, showing comparable ordering but somewhat faster motion than in the present study with plasma membrane vesicles.

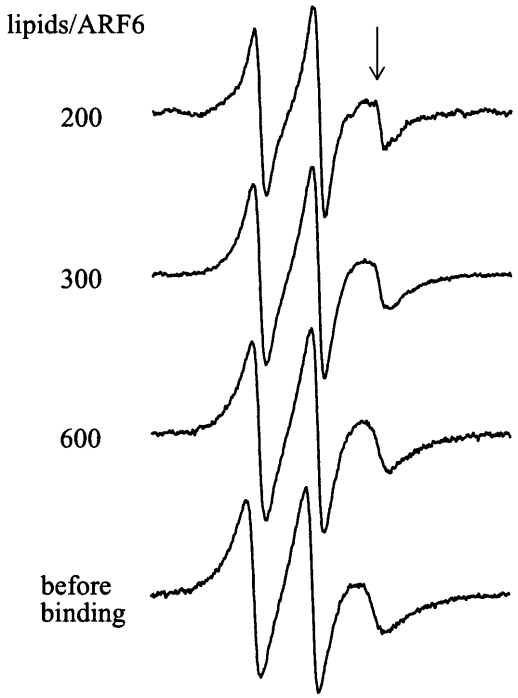

FIGURE 6 ESR spectra of DPPTC in the plasma membrane vesicles before and after ARF6 binding.

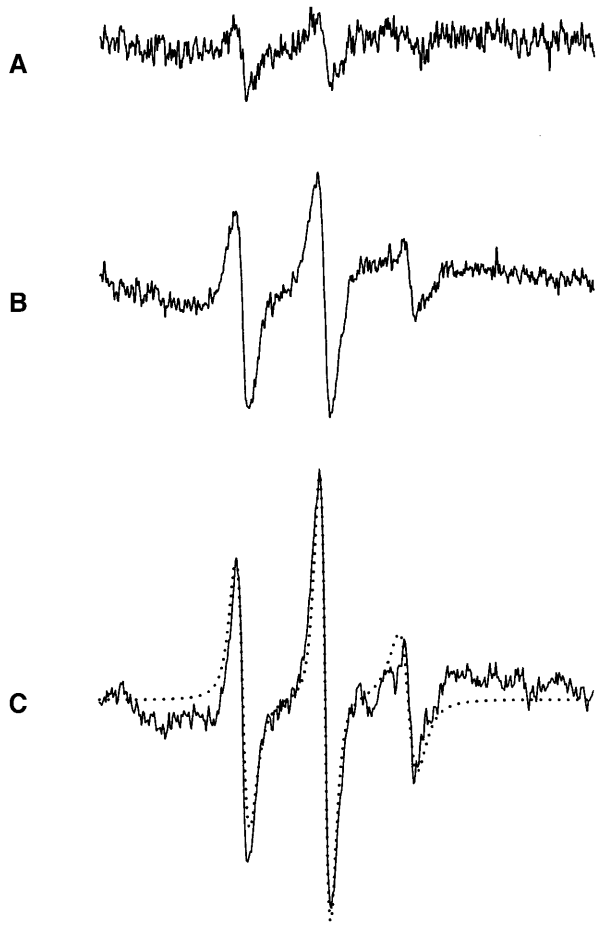

FIGURE 7 Difference spectra generated by subtracting the spectrum of DPPTC in plasma membrane vesicles before ARF6 binding from the spectra after ARF6 binding. *A*, *B*, and *C* are for cases of lipid/ARF6 ratio of 600, 300, and 200, respectively. The dotted line in *C* is the fit, as described in the text.

The success of the spectral subtraction also shows that upon incorporation of ARF6 into the membrane, the dominant, or broader, spectrum remains unaffected. Thus it is sufficient to just analyze the spectrum obtained before ARF6 binding. We initially attempted to fit this spectrum with a single component, but we could not obtain a satisfactory fit. In particular, the slow decay of the spectrum in its wings is difficult, if at all possible, to fit with just a single component. Such a feature is, however, consistent with the presence of more than one component. Unfortunately, this broad spectrum shows no distinct and unique features, clearly demonstrating more than one component, unlike the case of 5PC (cf. Fig. 2). Nevertheless, we found that it can be fit very well by using two components ($\chi^2_{\mathrm{red}} = 2.5$), but we do not have substantial confidence in the resulting fits, given this featureless spectrum. We briefly note the results: the more abundant component (67%) is relatively sharper with $R_\perp = 1.3 \times 10^8\ \mathrm{s}^{-1}$ and $S_0 = -0.12$, whereas the less abundant component (37%) is broader with $R_\perp = 2.8 \times 10^8\ \mathrm{s}^{-1}$ and $S_0 = 0.37$. These values of $R_\perp$ are larger than those obtained previously by cw-ESR for DPPTC in model membranes (Ge and Freed, 1998; Ge et al., 2001) or another headgroup label (SD-TEMPO) in DRM and in SM (Ge et al., 1999), where typically $R_\perp$ had a range of 2–6 $\times$ $10^7\ \mathrm{s}^{-1}$. The fact that S_0 for the two fitted components has opposite sign is not inconsistent with previous observations of SD-TEMPO in SM (Ge et al., 1999), where at 20°C it was 0.32 and at 50°C it became −0.23, nor of DPPTC in DPPC (Ge and Freed, 1998) where at 25°C it was 0.50 and −0.32 at 50°C. Thus the most straightforward interpretation of these results is that DPPTC is affected by heterogeneity in the lipid headgroups of the plasma membrane vesicles. By contrast, its spectrum is well fit by just a single component in the case of DRMs (Ge et al., 1999). The heterogeneity in the headgroup region may or may not be related to the heterogeneity observed with the acyl chain spin labels.

It is known that ARF6 is involved in cortical actin rearrangements (Radhakrishna et al., 1999), and ARF6 has been implicated in stimulated ruffling of RBL-2H3 cells (Holowka et al., 2001). Therefore, our observations of the changes in the DPPTC spectra upon ARF6 binding to plasma membrane vesicles suggests a mechanism by which ARF6 exerts its functional effects. Both ARF proteins and PIP_2 are important participants in the activation of phospholipase D1, which occurs at the plasma membrane after antigen stimulation in RBL-2H3 cells (Powner et al., 2002). The product of this enzyme, phosphatidic acid, has been shown to be a cofactor with ARF proteins in the activation of phosphatidyl inositol-4-phosphate-5-kinase 1α (Honda

et al., 1999). Production of newly synthesized PIP_2 by this latter enzyme provides sites for the initiation of actin polymerization (Tolias et al., 2000). Similarly, changes in glycerophospholipid composition were shown to initiate exocytosis in RBL-2H3 mast cells (Cohen and Brown, 2001; Ivanova et al., 2001) and a central role for phospholipase D in this process has been suggested. The mechanisms by which ARF GTPases participate in the activation of phospholipase D and phosphatidylinositol-4-phosphate-5-kinase are not yet clear, but our ESR results, which show large perturbations of the plasma membrane upon ARF6 binding, may suggest that changes in the structure of the surface (i.e., headgroup region) of the plasma membrane, including the formation of defects, may be a key event.

CONCLUSIONS AND FURTHER COMMENTS

Evidence is provided that liquid-ordered-like and liquid-crystalline-like phases or regions coexist in plasma membrane vesicles derived from RBL-2H3 cells. Proteins appear to play a role in stabilizing the coexistence of the two phases in the plasma membrane, and can also create defects in these membranes. These results may be relevant to the mechanisms by which IgE receptor cross-linking promotes segregation of these immunoreceptors into a liquid-ordered lipid environment that promotes receptor phosphorylation and the consequent initiation of signal transduction cascades (Holowka and Baird, 2001). Recent results indicate that segregation of cross-linked receptors, together with active Lyn tyrosine kinase, from a transmembrane phosphatase that prefers a more fluid membrane environment is critical for initiation of IgE receptor signaling (R. M. Young, D. Holowka, and B. Baird, unpublished results). The existence of discrete liquid-ordered and fluid phases in RBL plasma membranes, as found in the present study, provides physical evidence in support of this hypothesis.

We thank Ms. Norah Smith for preparation of plasma membrane vesicles, and Dr. Musti J. Swamy for helpful discussions.

This work was supported by National Institutes of Health grants GM-25862 and P41RR16292 (Jack H. Freed and Mingtao Ge), AI18306 (Barbara Baird and David Holowka), and GM58516 (H. Alex Brown), and by the Keck Foundation.

REFERENCES

Apgar, J. R., and M. F. Mescher. 1986. Protein and lipid composition of the detergent insoluble plasma membrane matrix of lymphoid cells. *In* Membrane Skeletons and Cytoskeletal-Membrane Associations. U. Bennett, C. M. Cohen, S. E. Lux, and J. Patek, editors. Alan R. Liss, New York. 293–305.

Barnes, J., and J. H. Freed. 1998. Dynamics and ordering in mixed model membranes of DMPC and DMPS: a 250-GHz ESR study using cholestane. *Biophys. J.* 75:2532–2546.

Budil, D. E., S. Lee, S. Saxena, and J. H. Freed. 1996. Nonlinear-least-squares analysis of slow-motion EPR spectra in one and two dimensions using a modified Levenberg-Marquardt algorithm. *J. Magn. Reson.* A120:155–189.

Cohen, J. S., and H. A. Brown. 2001. Phospholipases stimulate secretion in RBL mast cells. *Biochemistry.* 40:6589–6597.

Dietrich, C., L. A. Bagatolli, Z. N. Volovyk, N. L. Thompson, M. Levi, K. Jacobson, and E. Gratton. 2001. Lipid rafts reconstituted in model membranes. *Biophys. J.* 80:1417–1428.

Dietrich, C., B. Yang, T. Fijiwara, A. Kusumi, and K. Jacobson. 2002. Relationship of lipid rafts to transient confinement zones detected by single particle tracking. *Biophys. J.* 82:274–284.

Feigenson, G. W., and J. T. Buboltz. 2001. Ternary phase diagram of dipalmitoyl-PC/dilauroyl-PC/cholesterol: nanoscopic domain formation driven by cholesterol. *Biophys. J.* 80:2775–2788.

Field, K. A., D. Holowka, and B. Baird. 1995. Fc∈RI-mediated recruitment of $p53/56^{lyn}$ to detergent-resistant membrane domains accompanies cellular signaling. *Proc. Natl. Acad. Sci. USA.* 92:9201–9205.

Field, K. A., D. Holowka, and B. Baird. 1997. Compartmentalized activation of the high affinity immunoglobulin E receptor within membrane domain. *J. Biol. Chem.* 272:4276–4280.

Freed, J. H. 1994. Field gradient ESR and molecular diffusion in model membranes. *Annu. Rev. Biophys. Biomol. Struct.* 23:1–25.

Freed, J. H., A. Nayeem, and S. B. Rananavare. 1994. ESR and slow motions in liquid crystals. *In* The Molecular Dynamics of Liquid Crystals. G. R. Luckhurst and C. A. Veracini, editors. Kluwar, New York. 365–402.

Fridriksson, E. K., P. A. Shipkova, E. D. Sheets, D. Holowka, B. Baird, and F. W. McLafferty. 1999. Quantitative analysis of phospholipids in functionally important membrane domains from RBL-2H3 mast cells using tandem high-resolution mass spectroscopy. *Biochemistry.* 38: 8056–8063.

Ge, M., and J. H. Freed. 1993. An electron spin resonance study of interactions between gramicidin A′ and phosphatidylcholine bilayers. *Biophys. J.* 65:2106–2123.

Ge, M., and J. H. Freed. 1998. Polarity profiles in oriented and dispersed phosphatidylcholine bilayers are different: an electron spin resonance study. *Biophys. J.* 74:910–917.

Ge, M., and J. H. Freed. 1999. Electron-spin resonance study of aggregation of gramicidin in DPPC bilayers and hydrophobic mismatch. *Biophys. J.* 76:264–280.

Ge, M., D. E. Budil, and J. H. Freed. 1994. An electron spin resonance study of interaction between phosphatidylcholine and phosphatidylserine in oriented membrane. *Biophys. J.* 66:1515–1521.

Ge, M., J. S. Cohen, H. A. Brown, and J. H. Freed. 2001. ADP ribosylation factor 6 binding to phosphatidylinositol 4,5-bisphosphate-containing vesicles creates defects in the bilayer structure. an electron spin resonance study. *Biophys. J.* 81:994–1005.

Ge, M., K. A. Field, R. Aneja, D. Holowka, B. Baird, and J. H. Freed. 1999. Electron spin resonance characterization of liquid ordered phase of detergent-resistant membranes from RBL-2H3 cells. *Biophys. J.* 77:925–933.

Gidwani, A., D. Holowka, and B. Baird. 2001. Fluorescence anisotropy measurements of lipid order in plasma membranes and lipid rafts from RBL-2H3 mast cells. *Biochemistry.* 40:12422–12429.

Holowka, D., and B. Baird. 1983. Structural studies on the membrane-bound immunoglobulin E-receptor complex. 1. Characterization of large plasma membrane vesicles from rat basophilic leukemia cells and insertion of amphipathic fluorescent probes. *Biochemistry.* 22:3466–3474.

Holowka, D., and B. Baird. 2001. FcεRI as a paradigm for a lipid raft-dependent receptor in hematopoietic cells. *Semin. Immunol.* 13:1–7.

Holowka, D., H. A. Brown, A. Jeromin, and B. Baird. 2001. ARF GTPase and phosphatidylinositol-4-phosphate 5-Kinase 1a (PIP5K) participate in antigen-stimulated ruffling of RBL-2H3 mast cell. *Mol. Biol. Cell.* 12(Suppl.):1658. (Abstr.).

Honda, A., M. Nogami, T. Yokozeki, M. Yamazaki, H. Nakamura, H. Watanabe, K. Kawamoto, K. Nakayama, A. J. Morris, M. A. Frohman, and Y. Kanaho. 1999. Phosphatidylinositol 4-phosphate 5-kinase alpha is

a downstream effector of the small G protein ARF6 in membrane ruffle formation. *Cell*. 99:521–532.

Ivanova, P. T., B. A. Cerda, D. M. Horn, J. S. Cohen, F. W. McLafferty, and H. A. Brown. 2001. Electrospray ionization mass spectrometry analysis of changes in phospholipids in RBL-2H3 mastocytoma cells during degranulation. *Proc. Natl. Acad. Sci. USA*. 98:7152–7157.

Lee, A. G. 1988. Annular lipids and the activity of the calcium-dependent ATPase. *In* Lipid Domains and the Relationship to Membrane Function. R. C. Aloia, C. C. Curtain, and L. M. Gordon, editors. Alan R. Liss, New York.

Lou, Y., M. Ge, and J. H. Freed. 2001. A multifrequency ESR study of the complex dynamics of membranes. *J. Phys. Chem.* 105:11053–11056.

Powner, D. J., M. N. Hodgkin, and M. J. O. Wakelam. 2002. Antigen-stimulated activation of phospholipase D1b by Rac 1, ARF6, and PKCα in RBL-2H3 cells. *Mol. Biol. Cell.* 13:1252–1262.

Pralle, A., P. Keller, E. L. Florin, K. Simons, and J. K. Horber. 2000. Sphingolipid-cholesterol rafts diffuse as small entities in the plasma membrane of mammalian cells. *J. Cell Biol*. 148:997–1008.

Radhakrishna, H., O. Al-Awar, Z. Khachikian, and J. G. Donaldson. 1999. ARF6 requirement for Rac ruffling suggests a role for membrane trafficking in cortical actin rearrangements. *J. Cell Sci.* 112:855–866.

Raucher, D., T. Stauffer, W. Chen, K. Chen, S. Guo, J. D. York, M. P. Sheetz, and T. Mayer. 2000. Phosphatidylinositol 4,5-bisphosphate functions as a second messenger that regulates cytoskeleton-plasma membrane adhesion. *Cell*. 100:221–228.

Samsonov, A. V., I. Mihalyov, and F. S. Cohen. 2001. Characterization of cholesterol-sphingomyelin domains and their dynamics in bilayer membranes. *Biophys. J*. 81:1486–1500.

Schneider, D. J., and J. H. Freed. 1989. Calculating slow motional magnetic resonance spectra: a user's guide. *In* Spin Labeling Theory and Applications, Vol. 8. L .J. Berliner and J. Reuben, editors. Plenum Press, New York. 1–76.

Sedwick, C. E., and A. Altman. 2002. Ordered just so: Lipid rafts and lymphocyte function. www.stke.org/cgi/content/full/OC_sigtrans; 2002/122/re2.

Sheets, E. D., G. M. Lee, R. Simson, and K. Jacobson. 1997. Transient confinement of a glycosylphosphatidylinositol-anchored protein in the plasma membrane. *Biochemistry*. 36:12449–12458.

Simons, K., and D. Toomre. 2000. Functional rafts in cell membranes. *Nat. Rev. Mol. Cell Biol*. 387:569–572.

Swamy, M. J., and D. Marsh. 2001. Spin-label electron paramagnetic resonance studies on the interaction of avidin with dimyristoylphosphatidylglycerol membranes. *Biochim. Biophys. Acta*. 1513:122–130.

Swamy, M. J., M. Ramakrishnan, B. Angerstein, and D. Marsh. 2000. Spin-label electron spin resonance studies on the mode of anchoring and vertical location of the *N*-acyl chain in *N*-acylphosphatidylethanolamines. *Biochemistry*. 39:12476–12484.

Tolias, K. F., J. H. Hartwig, H. Ishihara, Y. I. Shibasaki, L. C. Cantley, and C. L. Carpenter. 2000. Type I_α phosphatidylinositol-4-phosphate 5-kinase mediates Rac-dependent actin assembly. *Curr. Biol*. 10:153–156.